

Supplemental Material: From Transient to Stationary Transport in Porous Networks under Various Adsorption Conditions and Kinetics

Daniela Bauer,^{*,†} Zaineb Zaafour,† Guillaume Batôt,† and Benoit Coasne[‡]

[†] IFP Energies Nouvelles, 1 & 4 Av. Bois Préau, 92852 Rueil Malmaison, France

[‡] Université Grenoble Alpes, CNRS, LIPhy, 38000 Grenoble, France

E-mail: daniela.bauer@ifpen.fr

1 Lattice Boltzmann TRT scheme for the resolution of Stokes equation

Lattice Boltzmann Method (LBM) is based on the discretization of the Boltzmann equation on a regular grid. Space and particle velocities are discretized and nodes are linked by the velocity vectors \mathbf{v}_q , $q \in [0, q_m]$ with $q_m = 8$. Particles only move with \mathbf{v}_q . Populations $f_q(\mathbf{r}, t)$ correspond to the particle density at position \mathbf{r} having the velocity \mathbf{v}_q . Lattice Boltzmann schemes consist of two specific steps to compute the evolution of the density of particles in time: the collision and propagation step.

Collision step In this step, population functions f_q are modified by means of the collision operator Ω , that takes a specific form depending on the equation of interest. The update of f_q is done as follows:

$$\tilde{f}_q(\mathbf{r}, t) = f_q(\mathbf{r}, t) + \Omega[f(\mathbf{r}, t)]_q. \quad (1)$$

Here, $\tilde{f}_q(\mathbf{r}, t)$ represents distributions after the collision step.

Propagation step In this step, the exchange of the population functions f_q between neighboring nodes is done with respect to the velocity set:

$$f_q(\mathbf{r} + \mathbf{v}_q \Delta t, t + \Delta t) = \tilde{f}_q(\mathbf{r}, t). \quad (2)$$

The collision operator of the LBM-TRT scheme, used in this article, comprises two relaxation rates, λ^+ and λ^- , specifying the symmetric and the anti-symmetric components. Symmetric parts are given by $f_q^+ = \frac{1}{2}(f_q + f_{\bar{q}})$ whereas anti-symmetric parts are defined as $f_q^- = \frac{1}{2}(f_q - f_{\bar{q}})$ with $q \in \{1, \dots, q_m/2\}$. $f_0^+ = f_0$ and $f_0^- = 0$ for $q = 0$.

λ^- is defined for all anti-symmetric non-equilibrium parts $n_q^- = f_q^- - e_q^-$ whereas λ^+ is defined for all symmetric non-equilibrium parts $n_q^+ = f_q^+ - e_q^+$. For the zero velocity equilibrium components are set as: $e_0^+ = e_0$ and $e_0^- = 0$.

Consequently, Eq. 1 can be written as:¹

$$\begin{aligned} \tilde{f}_q(\mathbf{r}, t) &= f_q(\mathbf{r}, t) + \lambda^+ n_q^+ + \lambda^- n_q^- \\ \tilde{f}_{\bar{q}}(\mathbf{r}, t) &= f_{\bar{q}}(\mathbf{r}, t) + \lambda^+ n_q^+ - \lambda^- n_q^- \\ \tilde{f}_0(\mathbf{r}, t) &= f_0(\mathbf{r}, t)(1 + \lambda^+) - \lambda^+ e_0 \end{aligned} \quad (3)$$

where $q \in \{1, \dots, q_m/2\}$. The LBM-TRT scheme is based on the definition of three parameters Λ^\pm and Λ to ensure numerical stability. Λ^\pm , Λ and λ^\pm are related as follows (¹):

$$\Lambda = \Lambda^+ \Lambda^- \quad (4)$$

where

$$\Lambda^\pm = -(1/2 + 1/\lambda^\pm) \quad (5)$$

and

$$-2 < \lambda^\pm < 0. \quad (6)$$

Stokes equation including the pressure gradient ∇P driving the flow is expressed as:

$$\begin{aligned} \nabla \mathbf{j} &= 0 \\ \nabla P &= \nu \Delta \mathbf{j} \end{aligned} \quad (7)$$

where \mathbf{j} represents the momentum. In the case of Stokes equation, equilibrium distributions e_q^\pm are given by:²

$$\begin{aligned} e_q^+(\mathbf{r}, t) &= v_s^2 \rho(\mathbf{r}, t) t_q^* \\ e_q^-(\mathbf{r}, t) &= t_q^* (\mathbf{j}(\mathbf{r}, t) \cdot \mathbf{v}_q) \\ e_0^+(\mathbf{r}, t) &= \rho(\mathbf{r}, t) - \sum_{q=1}^{q_m} e_q^+(\mathbf{r}, t) \\ e_0^- &= 0 \end{aligned} \quad (8)$$

Here, v_s represents the sound velocity. t_q^* are isotropic physical weights that follow two constraints:

$$\sum_{q=1}^{q_m} t_q^* \mathbf{v}_{q\alpha} \mathbf{v}_{q\beta} = \delta_{\alpha\beta} \quad \forall \alpha, \beta \quad (9)$$

and

$$\sum_{q=1}^{q_m} t_q^* \mathbf{v}_{q\alpha}^2 \mathbf{v}_{q\beta}^2 = \frac{1}{3} \quad \forall \alpha \neq \beta \quad (10)$$

where $\alpha, \beta \in \{1, 2\}$. $\delta_{\alpha\beta} = 0$ if $\alpha \neq \beta$ and $\delta_{\alpha\beta} = 1$ for $\alpha = \beta$.

In the d_2q_9 scheme, t_q^* are equal to $t_q^* = \{\frac{1}{3}; \frac{1}{12}\}$ for the first (coordinate) and the second (diagonal) neighbor link (²).

Equilibrium functions contain the momentum \mathbf{j} and the fluid density ρ . They can be computed from (²):

$$\rho(\mathbf{r}, t) = \sum_{q=0}^{q_m} f_q(\mathbf{r}, t) \quad (11)$$

and

$$\mathbf{j}(\mathbf{r}, t) = \sum_{q=1}^{q_m} f_q(\mathbf{r}, t) \mathbf{v}_q \quad (12)$$

Fluid velocity is calculated as $\mathbf{U}(\mathbf{r}, t) = \frac{\mathbf{j}(\mathbf{r}, t)}{\rho}$. The kinematic viscosity is given by $\nu = \frac{\Lambda^+}{3} = -\frac{1}{3}(\frac{1}{2} + \frac{1}{\lambda^+})$ and the pressure (Eq. 7) is expressed

as $P = v_s^2 \rho$. The adjustable positive parameter v_s must verify $v_s^2 < v_s^{max2}$ with $v_s^{max2} = \frac{1}{3}$.³ Here, in order to obtain numerical accuracy, we use the following values of the numerical parameters: $v_s^2 = \frac{1}{5}$, $\Lambda = 3/16$, $\nu = 1/10$, so $\Lambda^+ = 3/10$ and $\Lambda^- = 10/16$.

We apply the so-called bounce back rule at the solid/fluide interface given by: $f_q(\mathbf{r}, t + \Delta t) = f_q(\mathbf{r}, t)$. Further information on the inlet/outlet boundary conditions are presented in.⁴

2 Langmuir adsorption

In this section we present the results for slow adsorption kinetics ($k_L = 5$). Results are similar to those obtained for faster adsorption kinetics, but as we will show, the dispersion behavior takes place on a different time scale.

2.1 Influence of the initial concentration

Fig. S1 shows the normalized dispersion coefficient $D(t)/D_m$ [Top] and the corresponding skewness [Bottom] for the adsorption/desorption ratio $k_L = 5$ as a function of c_0 . $D(t)/D_m$ reaches a plateau for all initial concentrations c_0 . The slight increase in $D(t)/D_m$ for large t of high values of c_0 might be attributed to a boundary effect, where molecules start leaving the porous medium. Skewness is negative for all c_0 and it is lowest for high initial concentrations. Skewness values are very close to the value of the passive tracer. Negative skewness stands for a slight tailing for all initial concentrations that can be partially attributed to the porous structure and to the adsorption of a small amount of particles. The fact, that even for small values of c_0 , skewness is negative is due to the small adsorption rate k_A . The characteristic time to get adsorbed is higher, thus more molecules are subject to dispersion than for $k_A = 50$. Identically to the case of $k_L = 50$ the plateau of $D(t)/D_m$ increases with the initial concentration c_0 . Also, $D(t)/D_m$ is much smaller, particularly for high

values of c_0 , than in the case of $k_L = 50$.

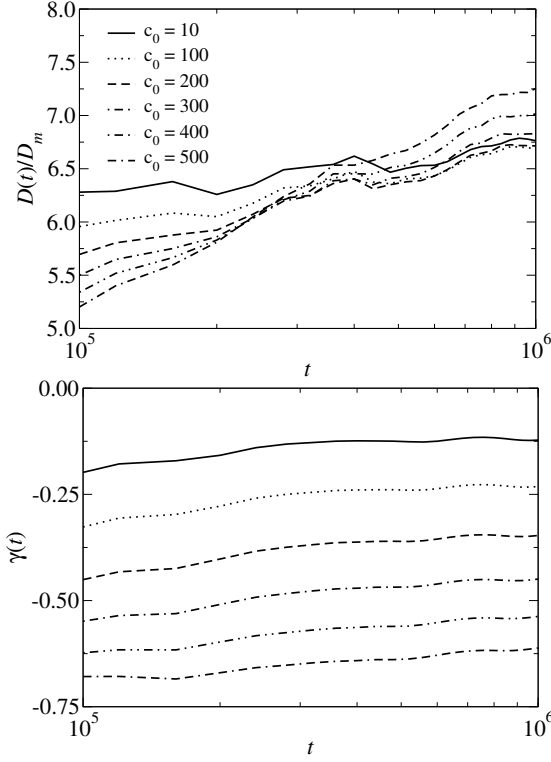


Figure S1: Results of Langmuir simulations for different initial concentrations c_0 , with $k_L = 5$, $\Gamma^\infty = 10$ and $Pe = 19$. The normalized dispersion coefficient $D(t)/D_m$ for different initial concentrations c_0 is represented in the top figure [Top], corresponding skewness [Bottom].

2.2 Influence of the surface saturation

Fig. S2 shows the temporal evolution of the dispersion coefficient $D(t)/D_m$ [Top] and the corresponding skewness [Bottom].

As can be seen, $D(t)/D_m$ reaches a plateau for all surface saturation Γ^∞ except for $\Gamma^\infty = 1$, where a very strong exponential increase can be observed.

For large values of Γ^∞ adsorption occurs without being limited by surface saturation; consequently, sampling between the adsorbed and desorbed states is efficient and the asymptotic regime is reached quickly after injection. In contrast, for small Γ^∞ , a strong increase in $D(t)/D_m$ can be observed that corresponds to the increase of $D(t)/D_m$ for $k_L = 50$ before the peak. Identically, as for $k_L = 50$ the strong

increase can be explained by the existence of two subpopulations: one part of the molecules is adsorbed rapidly after injection whereas the remaining molecules are transported by the Stokes velocity field. However, time to attain the equilibrium is much higher for small k_L . Thus, at the scale of the micromodel, a plateau cannot be reached for small values of Γ^∞ .

The skewness is slightly negative for large values of surface saturation, it becomes more negative with decreasing surface saturation and is lowest for $\Gamma^\infty = 1$. This can be explained by the fact that for smaller surface saturations adsorption is limited and a large part of free molecules are rapidly displaced by the velocity field. As the desorption kinetics are slow, adsorbed and then released molecules create tailing. For higher surface saturation the part of free molecules is lower, leading to higher values of skewness.

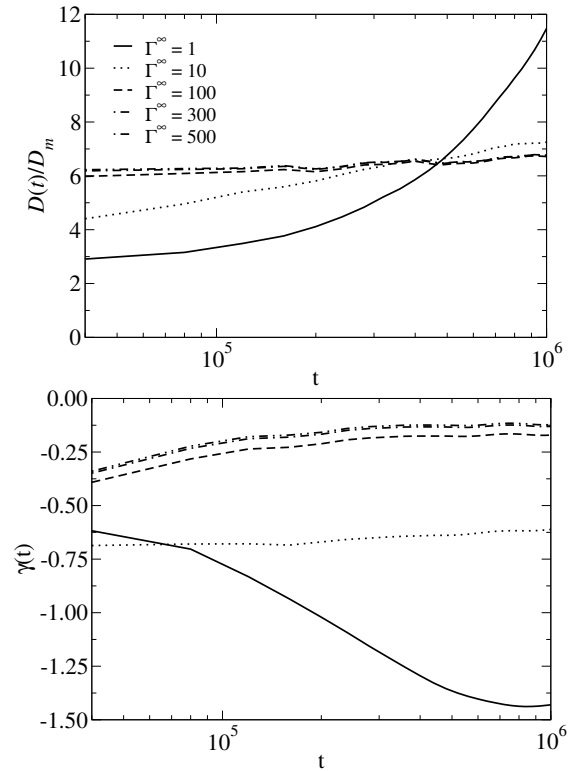


Figure S2: Results of Langmuir simulations for different maximum surface saturation Γ^∞ , with an initial concentration $c_0 = 500$, $k_L = 5$, $k_d = 0.001$, and $Pe = 19$. The normalized dispersion coefficient $D(t)/D_m$ [Top] and corresponding skewness [Bottom].

References

- (1) Ginzburg, I.; d’Humières, D.; Kuzmin, A. Optimal stability of advection-diffusion lattice Boltzmann models with two relaxation times for positive/negative equilibrium. *Journal of Statistical Physics* **2010**, *139*, 1090–1143.
- (2) Ginzburg, I. Lattice Boltzmann modeling with discontinuous collision components: Hydrodynamic and advection-diffusion equations. *Journal of Statistical Physics* **2007**, *126*, 157–206.
- (3) Ginzburg, I. Consistent lattice Boltzmann schemes for the Brinkman model of porous flow and infinite Chapman-Enskog expansion. *Physical Review E* **2008**, *77*, 066704.
- (4) Talon, L.; Bauer, D.; Gland, N.; Youssef, S.; Auradou, H.; Ginzburg, I. Assessment of the two relaxation time Lattice-Boltzmann scheme to simulate Stokes flow in porous media. *Water Resources Research* **2012**, *48*.